Regular Article

PHYSICAL CHEMISTRY RESEARCH
Published by the
Iranian Chemical Society
www.physchemres.org
info@physchemres.org

Phys. Chem. Res., Vol. 6, No. 1, 1-14, March 2018
DOI: 10.22036/pcr.2017.81787.1367

Chemisorption of Pyrimidine Nucleotide Onto Exterior Surface of Pristine $B_{12}N_{12}$ Nanocluster: A Theoretical Study

M. Solimannejad[a,b,*], S. Kamalinahad[c], M. Noormohammadbeigi[c] and H. Jouypazadeh[d]

[a]*Department of Chemistry, Faculty of Science, Arak University, 38156-8-8349, Arak, Iran*
[b]*Institute of Nanosciences and Nanotechnology, Arak University, 38156-8-8349, Arak, Iran*
[c]*Young Researcher and Elite Club, Arak Branch, Islamic Azad University, Arak, Iran*
[d]*Department of Chemistry, Isfahan University of Technology, Isfahan 84156-83111, Iran*
(Received 1 April 2017, Accepted 3 September 2017)

In this research, the interaction of pyrimidine molecule with pristine $B_{12}N_{12}$ nanocluster is studied in different phases to understand the effect of environment on the electronic properties of the designated adsorption complexes. To this end, the pyrimidine adsorption over $B_{12}N_{12}$ in the gas phase and water medium is investigated using density functional theory (DFT) at the B97D/6-31+G(d,p) level of theory. Must be said that the fragments and their both electronic and geometry structures are considered, and perturbation occurred by molecular adsorption will be interpreted through natural bond orbital (NBO) analysis. Our results confirm a chemical adsorption between pyrimidine molecule and exterior surface of pristine $B_{12}N_{12}$. One of the interesting features of this interaction is that pyrimidine adsorption in water medium is more favorable than that in the gas phase exhibiting an increase in adsorption energy (E_{ads}) compared to gas phase, from -120.44 to -141.85 kJ mol^{-1}. It is hoped that pristine $B_{12}N_{12}$ will be used in designing novel materials for potential applications in order to detect pyrimidine molecule in the gas phase and water medium.

Keywords: Pyrimidine, $B_{12}N_{12}$, Total density of state, Solvent effect

INTRODUCTION

Due to the presence of heterocyclic compounds in natural products such as vitamins, hormones, and antibiotics, these compounds play a critical role in daily life [1,2]. Therefore, there has been an on-going effort to develop a new generation of biologically active molecules [3,4]. Pyrimidine possesses two nitrogen atoms in a heterocyclic structure and it a biologically important compound [5]. Diazine family such as uracil, thiamine, and cytosine are some of the compounds derived from pyrimidine. Many natural products including vitamin B1 (thiamine), and synthetic compounds such as barbituric acid and Vernal, used as hypnotics, have pyrimidine skeleton in their structure [6]. Pyrimidines are important components of nucleic acids. They have been used in medical applications such as chemotherapy of AIDS as chemotherapeutic agents. Concerning the medicinal significant features of pyrimidines, it can be said that during the last two decades, several pyrimidine derivatives have been developed as chemotherapeutic agents and have found wide clinical applications. These compounds can be applied *in vitro* activity against unrelated DNA and RNA, antineoplastics and anticancer agents [7], drugs for hyperthyroidism [8], antibiotics [9], antitubercular drugs [10], viruses including polio herpes viruses, diuretic, antitumor, anti-AIDS, and cardiovascular [11-13]. The special features and applications of pyrimidine-like compounds make the medicinal chemists use it to generate the effective and innovative drug delivery systems based on nanostructures.

Nano based biomaterials are broadly used in medical

*Corresponding author. E-mail: m-solimannejad@araku.ac.ir

applications such as tissue engineering, biosensing, biological separation, molecular imaging and drug delivery. Drug delivery systems made up of nanostructures can significantly improve the drug treatment to the patient tissue as well as reducing the adverse effects of the drug on the healthy tissues. Incorporation of chemotherapeutic drugs and receptors specific for the target cells into nano carriers is a promising strategy in drug delivery area [14-16]. Nanoclusters are well-defined building blocks of the materials and devices with novel mechanical, electrical, and optical properties. As an application, we can refer to use nanoclusters as optical signal transducers of molecular binding, because of their significantly higher extinction coefficients compared to any organic and inorganic chromophores. The narrow size of distribution and surface ligand modification of nanoparticles allow them to be applied as transducers of biorecognition binding and molecular structure [17-19]. Different types of ″BN nanostructure″ compounds have been developed owning different characteristics including high-temperature stability, ultra-violet light emission, large thermal conductivity, oxidation resistance, and low dielectric constant [20-23]. This feature along with the toxicity of carbon containing materials allow us to investigate the performance of BN nanostructures in the biological systems as an alternative to the trouble-maker carbon components [24-26]. Therefore, B_nN_n clusters have been widely studied, both theoretically and experimentally, and $B_{12}N_{12}$ nanostructure appears to be more stable than the other compounds in the BN category [27,28]. Oku *et al*. [29] synthesized nanocage clusters of $B_{12}N_{12}$, which were detected by laser desorption time-of-flight mass spectrometry. They observed that tetragonal and hexagonal rings of BN have formed the structure of $B_{12}N_{12}$ cluster. The other interesting aspect regarding the BN nanostructures is the adsorption of biological molecules such as adenine, uracil, cytosine [30], urea [31], glycine [32], amino acid [33], DNA/RNA nucleobases [34] *etc*. Among these kinds of clusters studied recently [35-38], biosensing in medium solvent has attracted a particular attention. [39,40]. The use of solvent-sensitive has lately been extended to the design of biosensors to study biochemistry *in vitro* and in individual living cells. The abilities of biochemistry and molecular biology must be sometimes combined to produce a solvent-sensitive biosensor. In this study, we examine a possibility of pyrimidine molecular adsorption over the outer surface of $B_{12}N_{12}$ nanocluster in the gas phase and water medium, and report the results of density functional theory (DFT) calculations. Quantum mechanical and spectroscopic techniques such as natural bond orbital (NBO), reduce density gradient (RDG) and total density of states (TDOS) were used to look for the electronic perturbations arising from the adsorption procedure.

COMPUTATIONAL METHODS

Quantum mechanical calculations in this work were performed at the framework of density functional theory, being implemented in the Gaussian 09 program [41]. DFT is presently the most successful and promising approach to compute the electronic structure of matter. This method suggests the hope of tackling large systems in a broad context with a reasonable effort, and appears to be less basis set dependent compared to the more advanced wavefunction-based methods [42].

Recently, B97D as a specialized functional of DFT which can be scrutinized the treatment of van der Waals (dispersion) interactions has been developed [43]. So, this functional was assigned for modeling the molecular structures.

The basis sets for all atoms have a double-ζ quality augmented with one diffuse and two sets of polarization functions, 6-31+G(d,p). The correlated $<S^2>$ values are zero, verifying the pure singlet states. Vibrational frequency calculation was carried out on all fully optimized structures, pyrimidine molecule, $B_{12}N_{12}$ cluster, and their interacting complexes, to ensure a real minimum.

Since the pyrimidine molecule is usually found in water medium, solution effects were investigated using the polarizable continuum model (PCM) [44,45] with dielectric constant of 78.3553 for water. Therefore, geometry optimization procedure was done over all structures, fragments and complexes, using PCM model at the B97D/6-31+G(d,p) level. NBO analysis was also employed to provide insight into the charge transfer between the nanocage and adsorbed molecules [46].

Energy gap (E_g), Fermi level energy (E_F), and adsorption energy (E_{ads}) values as quantum molecular

descriptors [47] were computed. The energy gap has the following operational equation:

$$E_g = (E_{LUMO} - E_{HOMO}) \quad (1)$$

In this definition, E_{HOMO} and E_{LUMO} are the energy of the highest occupied and lowest unoccupied molecular orbitals, respectively. The conventional assumption for the Fermi level energy (E_F) is that it reclines approximately in the middle of the energy gap (E_g) at 0 K.

The adsorption energy (E_{ads}) of pyrimidine over the surface of pristine $B_{12}N_{12}$ is defined as,

$$E_{ads} = E_{complex} - E_{pyrimidine} - E_{BNnanocluster} + E_{BSSE} \quad (2)$$

where $E_{complex}$, $E_{pyrimidine}$, and $E_{BNnanocluster}$ are total energies of $B_{12}N_{12}$/pyrimidine complex, isolated pyrimidine, and pristine $B_{12}N_{12}$, respectively. In order to eliminate effects of basis functions overlap, the basis set superposition error (BSSE) was applied using counterpoise method [48]. According to the Eq. (2), negative adsorption energy correlates to the stability of interacting complex.

Total density of states (TDOS) and partial density of states (PDOS) analyses were performed on the pristine fragments and $B_{12}N_{12}$/pyrimidine complex at the same level of theory using the GaussSum program [49].

RDG was also used to characterize the non-covalent interactions. The dimensionless RDG (s) is evaluated from the density (ρ) and its first derivative [50], RDG = $(1/(2(3\pi^2)^{1/3}))$ $((|\nabla\rho|)/\rho^{4/3})$. Density values give just information about the strength of interaction and do not classify them as attractive or repulsive interactions. For this purpose, the sign of the second eigenvalue (λ_2) of the electron density Hessian matrix is considered to distinguish between different types of non-covalent interactions, *i.e.*, hydrogen bonding, van der Waals interactions, and steric repulsion. So, electron density increased with λ_2 sign is used as a descriptor for the nature of interacting bonds; $\Omega = \text{sign}(\lambda_2)\rho$. MULTIWFN [51] software was also used to draw the non-covalent interaction (NCI) plots, RDG versus $\text{sign}(\lambda_2)\rho$. Low-density and low-gradient spikes associated with density located between interacting paths are as signature of non-covalent interactions.

RESULTS AND DISCUSSION

Geometry Optimization and Structure of Pristine $B_{12}N_{12}$ in Gas Phase and Water Medium

The optimized structures of pristine $B_{12}N_{12}$ and pyrimidine at the B97D/6-31+G(d,p) level of theory in the gas phase are shown in Fig. 1a and 1b. The optimized geometry of pyrimidine molecule is in conformity with experimental studies [52]. Figure 1a reveals that two individual bonds in $B_{12}N_{12}$ are recognizable; one of them is shared between a tetragonal and a hexagon ring and the other one is placed between two hexagon rings. The calculated lengths of these bonds are 1.494 and 1.450 Å, respectively. These results are in good agreement with the previous reports [53].

The electronic properties of pristine BN cluster are studied through NBO analysis. NBO-based computation demonstrates that natural charge over N atom in $B_{12}N_{12}$ is about -1.148 |e|. The electronegativity difference between boron and nitrogen atoms causes an ionic B-N bond formation which is proved by the NBO analysis. As a further support for the reliability of our optimization procedure, we take a look at the frontier molecular orbital energies (E_{HOMO} and E_{LUMO}) and E_g values for the considered nanocluster, listed in Table 1. The obtained energy gap quantity for the $B_{12}N_{12}$ is about 5.12 eV which are comparable with those reported in the other DFT studies [54,55]. Moreover, TDOS and graphic presentation of the HOMO and LUMO distribution for $B_{12}N_{12}$ are presented in Fig. 1c.

Pyrimidine is one of the most common molecules in the biological systems; therefore, investigation of the solution effects on the adsorption ions is in order. The optimization procedure for $B_{12}N_{12}$ and pyrimidine is done with imposing polarizable continuum model (PCM) in water medium, and their structures are shown in Fig. 2a and b. As inferred from Fig. 2a, there is no clear difference between the bond lengths in the gas phase and water medium.

The electronic properties of this nanocluster are also listed in Table 1. The value of energy gap for $B_{12}N_{12}$ is observed about 5.18 eV which is increased with respect to the corresponding quantities in the gas phase. TDOS and graphic presentation of the HOMO and LUMO distribution of pristine $B_{12}N_{12}$ in water medium, presented in Fig. 2c,

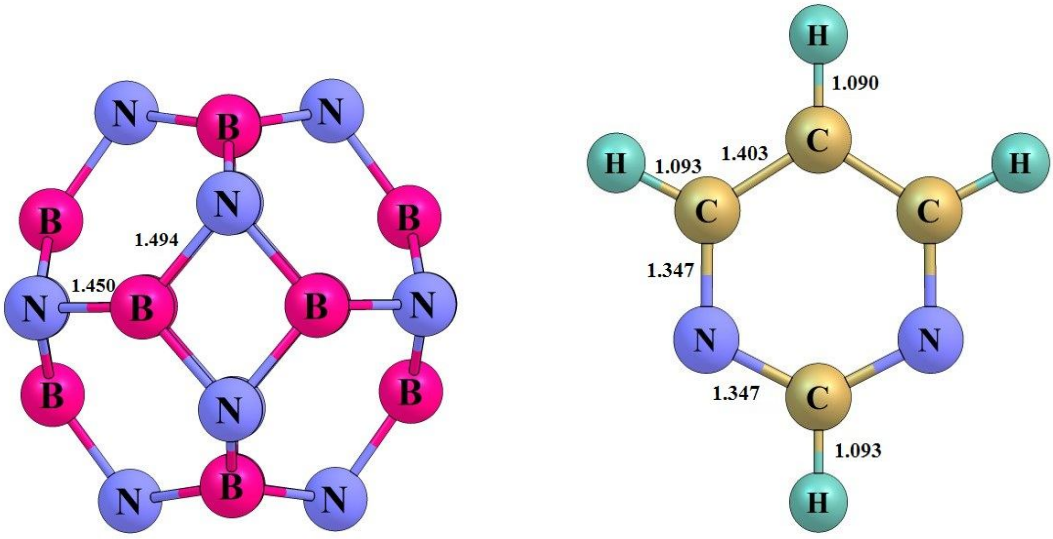

(a) **(b)**

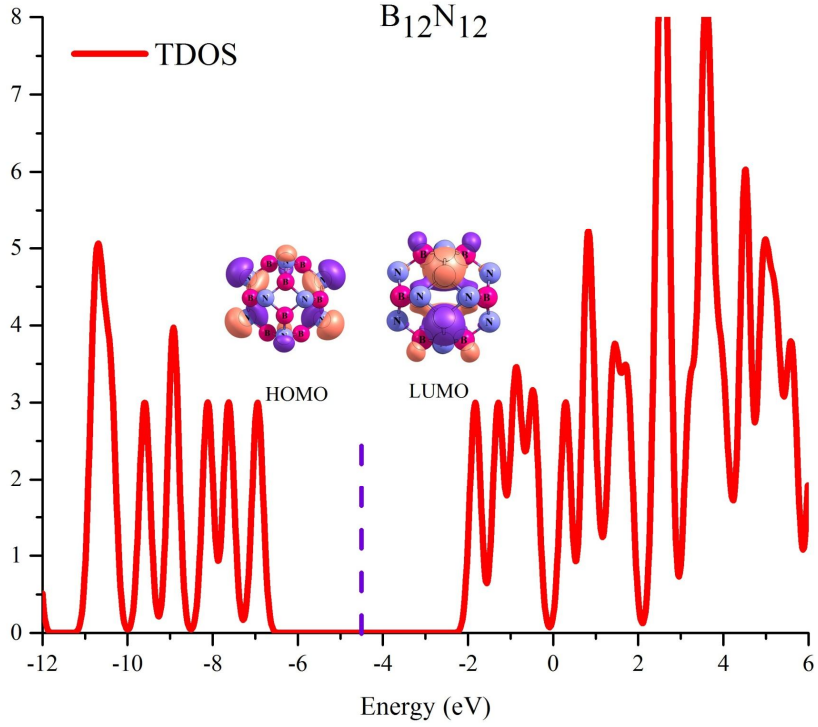

(c)

Fig. 1. Optimized structure of (a) $B_{12}N_{12}$ (b) pyrimidine and (c) total density of states (TDOS) of $B_{12}N_{12}$ in the gas phase (Bonds in Å). The dashed line in TDOS plots indicates Fermi energy.

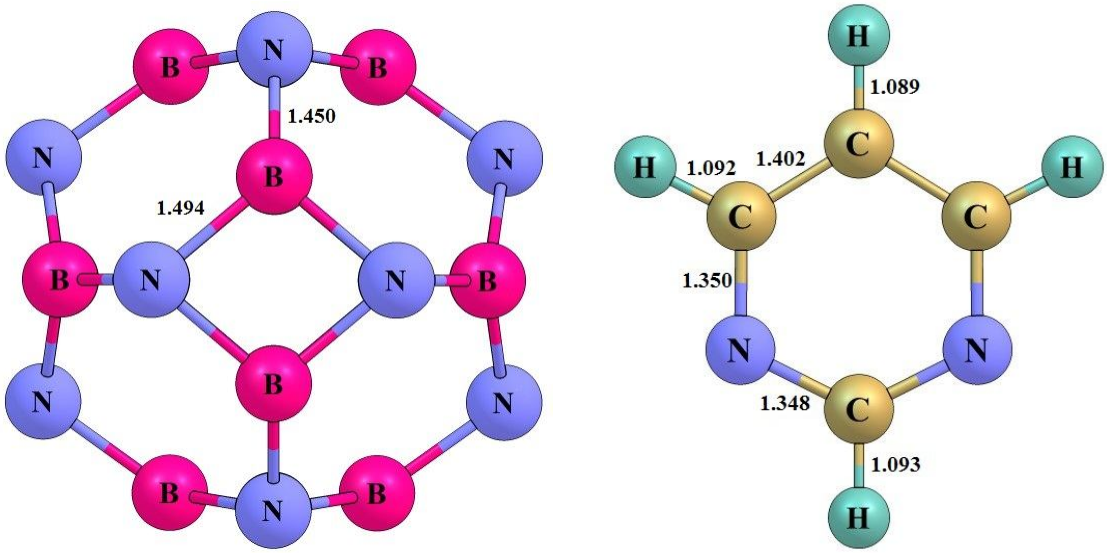

(a) **(b)**

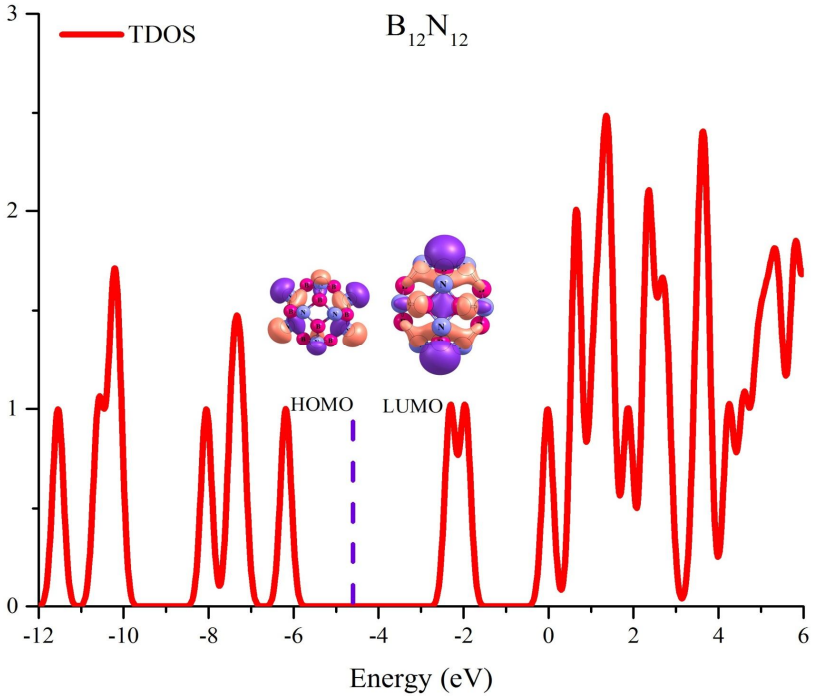

(c)

Fig. 2. Optimized structure of (a) pristine $B_{12}N_{12}$, (b) pyrimidine and (c) total density of states (TDOS) of pristine $B_{12}N_{12}$ in water medium (Bonds in Å). The dashed line in TDOS plots indicates Fermi energy.

Table 1. The Highest Occupied Molecular Orbital Energy (E_{HOMO}), Lowest Unoccupied Orbital Energy (E_{LUMO}), Energy Gap (E_g), the Change of Energy Gap of Nanocluster after Adsorption (ΔE_g (%)), Fermi Level Energies (E_F), Charge Transfer from Molecule to Cluster (Q_T), Adsorption Energy (E_{ads}) and BSSE Calculated for Pristine $B_{12}N_{12}$ and $B_{12}N_{12}$/Pyrimidine Complex in Gas Phase and Water Medium

	Configuration	E_{HOMO} (eV)	E_{LUMO} (eV)	E_g (eV)	ΔE_g (%)	E_F (eV)	Q_T (me)	E_{ads} (kJ mol^{-1})	BSSE (kJ mol^{-1})
Gas	$B_{12}N_{12}$	-6.94	-1.82	5.12	-	-4.38	-	-	-
Phase	$B_{12}N_{12}$/pyrimidine	-6.05	-3.87	2.18	-57.34	-4.96	334	-120.44	8.42
Water	$B_{12}N_{12}$	-6.90	-1.72	5.18	-	-4.31	-	-	-
Medium	$B_{12}N_{12}$/pyrimidine	-6.23	-3.29	2.94	-43.27	-4.76	369	-141.85	-

Table 2. The Second-order Perturbation Energy E(2) Values (kcal mol^{-1}), the Donor-acceptor (Bond-antibond) Interactions for the $B_{12}N_{12}$/pyrimidine Complexes in the Gas Phase and Water Medium

	Donor NBO	Acceptor NBO	E(2)
Gas Phase	BD (1) B9-N29	BD*(1) C25-N29	2.15
	BD (1) B9-N29	BD*(1) C25-N34	4.90
	BD (1) B9-N29	BD*(1) C27-C28	3.48
	BD (1) B9-N29	BD*(1) C28-N29	2.13
	BD* (1) B9-N29	BD*(1) C25-N29	1.08
Water Medium	BD (1) B9-N29	BD*(1) C25-N29	2.28
	BD (1) B9-N29	BD*(1) C25-N34	4.69
	BD (1) B9-N29	BD*(1) C27-C28	3.10
	BD (1) B9-N29	BD*(1) C28-N29	2.25

illustrates the HOMO is concentrated on the N atoms of the nanocluster while the LUMO is spread over the B atoms.

Pyrimidine Adsorption on Pristine $B_{12}N_{12}$ in Gas Phase and Water Medium

The second stage is determining the electrostatic charge distribution over fragments and detecting the effective forces in the formation of an adsorbing complex. Therefore, we search for a suitable position on the exterior surface of pristine $B_{12}N_{12}$ for the molecular adsorption of pyrimidine. For this purpose, a pyrimidine molecule is initially placed at different positions on the exterior surface of $B_{12}N_{12}$ with various orientations. After full geometry optimization, the most stable adsorption configuration in the real minimum is found (see Fig. 3a). In this configuration, the nitrogen atom of pyrimidine molecule is closed to a B atom of the external surface of $B_{12}N_{12}$ cluster with an interaction distance of 1.642 Å. The calculated E_{ads} and BSSE values for $B_{12}N_{12}$/pyrimidine complex are computed by Eq. (2) and tabulated in Table 1. E_{ads} value for this configuration for the pyrimidine adsorption in the gas phase is -120.44 kJ mol^{-1} indicating that chemisorption process is occurred between pyrimidine molecule and $B_{12}N_{12}$.

NBO analysis shows a charge transfer of 334 |me| from pyrimidine molecule to $B_{12}N_{12}$ nanocluster, confirming chemical adsorption. Electron transfer from the lone pair orbital located on N atoms to the empty p orbital of B leads to the non-covalent interaction between the BN nanocluster and pyrimidine, which has an important role in stabilization of the system. Additionally, the second-order perturbative estimates of donor-acceptor (bond-antibond) interactions in the NBO basis were studied. All possible interactions between filled (donor) Lewis-type NBOs and empty (acceptor) non-Lewis NBOs are examined and their energetic importance is investigated by 2nd-order perturbation theory [56-59].

The most important interactions for the most stable configuration are presented in Table 2. It is obvious from this table that the strongest interaction corresponds to the interaction of σ-bond B9-N29 localized on $B_{12}N_{12}$/pyrimidine complex as donor with the adjacent π* (C25-N34) with the energy 4.90 kcal mol^{-1}.

A visualization analysis of the non-covalent interactions was made to understand the nature of non-bonding interactions in $B_{12}N_{12}$/pyrimidine complex. According to Yang *et al*., large negative values of sign $(\lambda_2)\rho$ in the two-dimensional RDG plots represent attractive interactions (*e.g*., hydrogen bonding) whereas large positive values of sign $(\lambda_2)\rho$ show steric repulsion.

On the other hand, the values close to zero (in the low density region) represent van der Waals interaction. Scatter graph of $B_{12}N_{12}$/pyrimidine, illustrated in Fig. 3c, shows that there are several spikes for $B_{12}N_{12}$/pyrimidine configuration (see Fig. 3c). In each region, more scatter points display larger electron density, that is, larger contribution to total weak interactions. According to Fig. 3c, disperse spikes near sign (λ_2) ρ = -0.01 a.u. can be settled within the regions of the isosurface with deep blue equivalent to stabilizing interactions, *viz*., N29-B9, reflective attractions. While, a red space corresponding to the scatter plots with more than -0.01 a.u. for sign (λ_2) ρ indicates a weak repulsive interaction between the pyrimidine and exterior surface $B_{12}N_{12}$ nanocluster.

The adsorption process leads to a local structural deformation of both fragments, in particular, N-C bond length elongation from 1.347 Å in free pyrimidine molecule to 1.351 Å in the complex of $B_{12}N_{12}$/pyrimidine and C-C bond length decrement from 1.403 Å to 1.402 Å of pyrimidine through the adsorption. Moreover, the B-N bonds of $B_{12}N_{12}$ are increased from 1.450 and 1.494 Å in the pristine form to 1.462 and 1.496 Å in the $B_{12}N_{12}$/pyrimidine complex (see Fig. 3a).

This section shows how perturbation in the electronic properties can be an important aspect of the adsorption process. We study the effects of pyrimidine molecular adsorption on the electronic properties of the $B_{12}N_{12}$ nanocluster (see Table 1). Through the adsorption process of pyrimidine on the exterior surface of $B_{12}N_{12}$ nanocluster, the energy gap of the $B_{12}N_{12}$/pyrimidine complex is found to be 2.18 eV. Based on the HOMO, LUMO, and TDOS visualizations for $B_{12}N_{12}$/pyrimidine complex (presented in Fig. 3b), HOMO is more located on nanocluster in $B_{12}N_{12}$/pyrimidine complex, while LUMO in this interacting system is remained over the pyrimidine molecule. This figure also confirms that the adsorption of pyrimidine molecule is accompanied by a significant change near the conduction level compared with pristine $B_{12}N_{12}$. To provide a sensible justification for the electronic properties

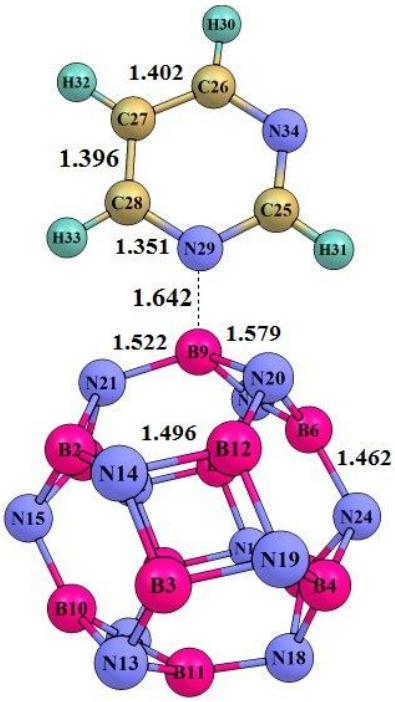

(a)

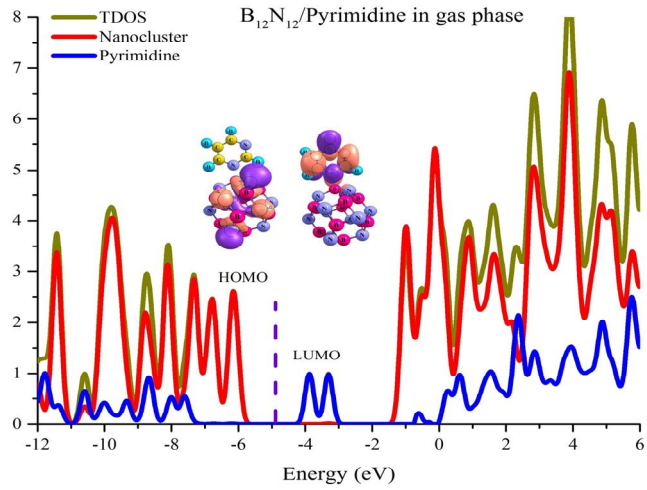

(b)

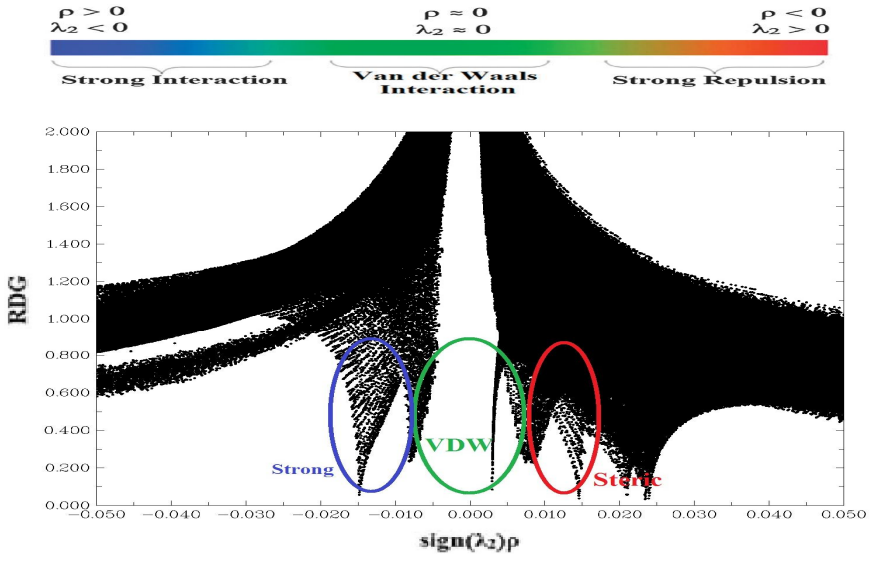

(c)

Fig. 3. (a) Optimized structures, (b) total density of states (TDOS) and partial density of states (PDOS) of the $B_{12}N_{12}$/Pyrimidine complex in the gas phase. The dashed line in PDOS plots indicates Fermi energy and (c) and plot of the reduced density gradient (RDG) versus sign $(\lambda_2)\rho$ (isovalue = 0.5 a.u.). (Bonds are in Å and angles in degree).

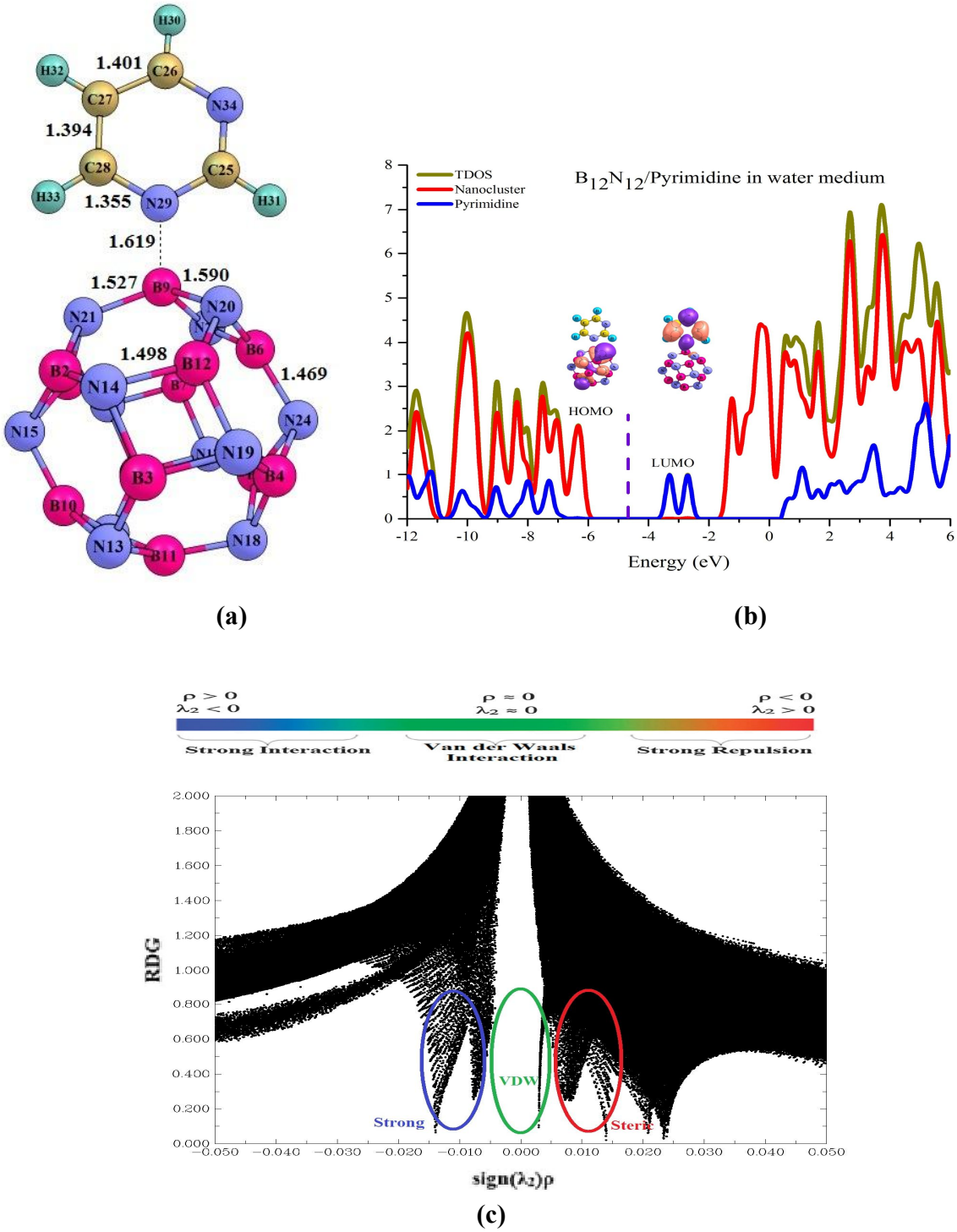

Fig. 4. (a) Optimized structures, (b) total density of states (TDOS) and partial density of states (PDOS) of the $B_{12}N_{12}$/Pyrimidine complex in water medium. The dashed line in PDOS plots indicates Fermi energy and (c) plot of the reduced density gradient (RDG) versus sign $(\lambda_2)\rho$ (isovalue = 0.5 a.u.). (Bonds are in Å and angles in degree).

perturbation of the $B_{12}N_{12}$/pyrimidine complex, we analyze PDOS, Fig. 3b, as a further understanding of the individual contribution of species to the Fermi energy region. Red and blue lines in Fig. 3b represent partial density of states of nanocluster and pyrimidine, respectively. It reveales that the PDOS of pyrimidine lies near the Fermi energy after the adsorption process, and can change the electronic properties of $B_{12}N_{12}$ near Fermi energy (Fig. 3b). In addition, the band gap of the $B_{12}N_{12}$/pyrimidine complex decreases by 57.34%, and consequently, the conductivity of the system is changed. Based on reported results, nanocluster can be sensitive enough to sense of pyrimidine molecule.

Stable configuration for the interacting system in the gas phase, obtained from previous sections, is reoptimized using PCM with dielectric constant of 78.3553 for water (see Fig. 4a). In this configuration, interaction distance between nitrogen atom in the pyrimidine molecule and B atom of the external surface of the $B_{12}N_{12}$ cluster is 1.619 Å. The calculated E_{ads} value for $B_{12}N_{12}$/pyrimidine complex without considering BSSE is -141.85 kJ mol^{-1}. This result reveals that pyrimidine molecule is chemisorbed onto $B_{12}N_{12}$ in water medium. The calculated NBO charges indicate that the charge transfer of 369 |me| is occurred from pyrimidine molecule to $B_{12}N_{12}$ nanocluster, confirming chemisorptions adsorption. The main interaction between the BN nanocluster and pyrimidine in water medium is due to charge transfer from the lone pair orbital of the N atom in pyrimidine to the empty p orbital over the B atom of the nanocluster. Moreover, the second-order perturbative estimates of donor-acceptor (bond-antibond) interactions in the NBO basis are investigated in water medium (See Table 2). It is obvious from this table that the strongest interaction corresponds to the interaction of σ-bond B9-N29 localized on $B_{12}N_{12}$/pyrimidine complex as donor with the adjacent π* (C25-N34) with the energy 4.69 kJ mol^{-1}.

RDG scatter graph of $B_{12}N_{12}$/pyrimidine in water medium is shown in Fig. 4c. The spikes with values near 0.01 a.u. arise from the relatively strong interaction between the nitrogen atom in the pyrimidine molecule and B atom of the $B_{12}N_{12}$ cluster. In addition, the spikes with values near -0.01 a.u. arise from the weak repulsive interaction between the pyrimidine and exterior surface $B_{12}N_{12}$ nanocluster.

The adsorption process leads to a local structural deformation in both fragments. The N-C bond length is elongated from 1.349 Å in free pyrimidine molecule to 1.355 Å in the complex, while C-C bond length is decreased from 1.402 Å to 1.401 Å for the corresponding systems. Moreover, the B-N bonds of the $B_{12}N_{12}$ are increased from 1.450 and 1.494 Å in the pristine form to 1.469 and 1.498 Å in the $B_{12}N_{12}$/pyrimidine complex (see Fig. 4a).

We study the effects of pyrimidine molecular adsorption on the electronic properties of the $B_{12}N_{12}$ nanocluster in water medium through E_g and E_F calculations (see Table 1). Upon the adsorption process in water medium, E_g of $B_{12}N_{12}$/pyrimidine complex is found to be 2.94 eV. The HOMO, LUMO and TDOS calculations are also performed for this configuration, Fig. 4b. According to this figure, the HOMO is located on nanocluster in the $B_{12}N_{12}$/pyrimidine complex while the LUMO is remained on the pyrimidine molecule. It can be seen that after adsorption process in water medium, a substantial change near the conduction level compared to that of the pristine $B_{12}N_{12}$ is appeared. PDOS changes reported for the BN cluster through the adsorption process in water medium (see Fig. 4b) reveales that the PDOS of pyrimidine molecule is close to the Fermi energy, and therefore can alter the electronic properties of $B_{12}N_{12}$ near the Fermi energy. For this reason, the band gap of the $B_{12}N_{12}$/pyrimidine complex shows 43.27% decrement, and the conductivity of the system is changed. Based on the mention results, this nanocluster is sensitive enough for sensing of pyrimidine molecule.

In the end, based on the DFT calculations, we have found that the electronic properties of $B_{12}N_{12}$ nanocluster interacting with pyrimidine molecule are changed significantly. Our study indicates that the adsorption energy of pyrimidine in the exothermic process is negative. The reported results in the previous study for the adsorption of 5-fluorouracil molecule on the surface of $B_{12}N_{12}$ are in consistence with the present results [60]. Therefore, $B_{12}N_{12}$ nanocluster is proposed for using as a recognition tool of nucleotide such as pyrimidine.

CONCLUSIONS

In this article, we have used density functional theory calculation to investigate the adsorption of pyrimidine molecule onto pristine $B_{12}N_{12}$ in the gas phase and water medium. The geometrical structures, electronic properties,

and NBO analysis for BN cluster have been performed in the presence and absence of a pyrimidine molecule to predict the electronic changes through the adsorption process. The obtained results exhibited that pyrimidine molecule interacts with the pristine $B_{12}N_{12}$ through strong interactions which imply to chemisorptions process. The interaction between $B_{12}N_{12}$ and pyrimidine in water medium is stronger than in the gas phase with considerable changes in its electrical conductance. Accordingly, $B_{12}N_{12}$ is introduced as a promising nano sensor to detect pyrimidine due to some features such as high sensitivity and also energetic favorability.

REFERENCES

[1] Ju, Y.; Kumar, D.; Varma, R. S., Revisiting nucleophilic substitution reactions: microwave-assisted synthesis of azides, thiocyanates, and sulfones in an aqueous medium. *J. Org. Chem.* **2006**, *71*, 6697-6700. DOI: 10.1021/jo061114h.

[2] Ju, Y.; Varma, R. S., Aqueous N-heterocyclization of primary amines and hydrazines with dihalides: microwave-assisted syntheses of N-azacycloalkanes, isoindole, pyrazole, pyrazolidine, and phthalazine derivatives. *J. Org. Chem*. **2006**, *71*, 135-141. DOI: 10.1021/jo051878h.

[3] Lokhande, P.; Waghamare, B.; Sakate, S., Regioselective one-pot synthesis of 3,5-diaryl-pyrazoles. *Indian J. Chem. Sect. A* **2005**, *44*, 2338-2342.

[4] Haino, T.; Tanaka, M.; Ideta, K.; Kubo, K.; Mori, A.; Fukazawa, Y., Solid-phase synthesis of liquid crystalline isoxazole library. *Tetrahedron lett.* **2004**, *45*, 2277-2279. DOI:10.1016/j.tetlet.2004.01.116.

[5] Elguero, J., Comprehensive Heterocyclic Chemistry. Karitzyky, AR 1984, pp. 167-303.

[6] Porter, A., Diazines and Benzodiazines, Vol. 14. 1979. Pregamon Press, Elsevier Science BV, Amsterdam, The Netherlands.

[7] Al Safarjalani, O. N.; Zhou, X.-J.; Rais, R. H.; Shi, J.; Schinazi, R. F.; Naguib, F. N., el Kouni, M. H., 5-(Phenylthio) acyclouridine: a powerful enhancer of oral uridine bioavailability: relevance to chemotherapy with 5-fluorouracil and other uridine rescue regimens. *Cancer Chemother. Pharmacol.* **2005**, *55*, 541-551.

[8] Roth, B.; Cheng, C., 6 Recent progress in the medicinal chemistry of 2, 4-diaminopyrimidines. *Prog. Med. Chem*. **1982**, 19269-331. DOI: 10.1016/S0079-6468(08)70332-1.

[9] Reddick, J. J.; Saha, S.; Lee, J. -M.; Melnick, J. S.; Perkins, J.; Begley, T. P., The mechanism of action of bacimethrin, a naturally occurring thiamin antimetabolite. *Bioorg. Med. Chem. Lett.* **2001**, *11*, 2245-2248. DOI: 10.1016/S0960-894X(01)00373-0.

[10] Nomoto, S.; Teshima, T.; Wakamiya, T.; Shiba, T., The revised structure of capremmycin. *J. Antibiot.* **1977**, *30*, 955-959. DOI: 10.7164/antibiotics.30.955.

[11] Oliver Kappe, C., 100 years of the biginelli dihydropyrimidine synthesis. *Tetrahedron* **1993**, *49*, 6937-6963. DOI: 10.1016/S0040-4020(01)87971-0.

[12] Rodrigues, A.; Rosa, J.; Gadotti, V.; Goulart, E.; Santos, M.; Silva, A.; Sehnem, B.; Rosa, L.; Gonçalves, R.; Corrêa, R., Antidepressant-like and antinociceptive-like actions of 4-(4′-chlorophenyl)-6-(4″-methylphenyl)-2-hydrazinepyrimidine mannich base in mice. *Pharmacol. Biochem. Behav*. **2005**, *82*, 156-162. DOI: 10.1016/j.pbb.2005.08.003.

[13] Xie, F.; Zhao, H.; Zhao, L.; Lou, L.; Hu, Y., Synthesis and biological evaluation of novel 2,4,5-substituted pyrimidine derivatives for anticancer activity. *Bioorg Med. Chem. Lett*. **2009**, *19*, 275-278. DOI: 10.1016/j.bmcl.2008.09.067.

[14] Duncan, R., Polymer conjugates as anticancer nanomedicines. *Nature Rev. Cancer* **2006**, *6*, 688-701. DOI: 10.1038/nrc1958.

[15] Ferrari, M., Cancer nanotechnology: opportunities and challenges. *Nat. Rev. Cancer* **2005**, *5*, 161-171. DOI: 10.1038/nrc1566.

[16] Silva, G. A., Neuroscience nanotechnology: progress, opportunities and challenges. *Nat. Rev. Neurosci.* **2006**, *7*, 65-74. DOI: 10.1038/nrn1827.

[17] Bromann, K.; Giovannini, M.; Brune, H.; Kern, K., Self-organized growth of cluster arrays. *EPJD* **1999**, *9*, 25-28. DOI: 10.1007/s100530050393.

[18] Mayer, C.; Stich, N.; Palkovits, R.; Bauer, G.; Pittner, F.; Schalkhammer, T., High-throughput assays on the chip based on metal nano-cluster resonance

transducers. *J. Pharm. Biomed. Anal*. **2001**, *24*, 773-783. DOI: 10.1016/S0731-7085(00)00545-8.

[19] Mayer, C.; Verheijen, R.; Stich, N.; Schalkhammer, T. G., Food-allergen assays on chip based on metal nano-cluster resonance. In: BiOS 2001 The International Symposium on Biomedical Optics, 2001. International Society for Optics and Photonics, pp. 134-141.

[20] Chopra, N. G.; Luyken, R.; Cherrey, K.; Crespi, V. H.; Cohen, M. L.; Louie, S. G.; Zettl, A., Boron nitride nanotubes. *Science* **1995**, *269*, 966-967. DOI: 10.1126/science.269.5226.966.

[21] Rogers, K.; Fowler, P.; Seifert, G., Chemical versus steric frustration in boron nitride heterofullerene polyhedra. *Chem. Phys. lett.* 2000, *332*, 43-50. DOI:10.1016/S0009-2614(00)01234-3.

[22] Sun, Q., Wang, Q., Jena, P., Storage of molecular hydrogen in BN cage: Energetics and thermal stability. *Nano Lett.* **2005**, *5*, 1273-1277. DOI: 10.1021/nl050385p.

[23] Wu, H.; Fan, X.; Kuo, J. -L., Metal free hydrogenation reaction on carbon doped boron nitride fullerene: A DFT study on the kinetic issue. *Int. J. Hydrogen Energy* **2012**, *37*, 14336-14342. DOI: 10.1016/j.ijhydene.2012.07.081.

[24] Cui, D.; Tian, F.; Ozkan, C. S.; Wang, M.; Gao, H., Effect of single wall carbon nanotubes on human HEK293 cells. *Toxicol. Lett.* **2005**, *155*, 73-85. DOI: 10.1016/j.toxlet.2004.08.015.

[25] Magrez, A.; Kasas, S.; Salicio, V.; Pasquier, N.; Seo, J. W.; Celio, M.; Catsicas, S.; Schwaller, B.; Forró, L., Cellular toxicity of carbon-based nanomaterials. *Nano Lett.* **2006**, *6*, 1121-1125. DOI: 10.1021/nl060162e.

[26] Bottini, M.; Bruckner, S.; Nika, K.; Bottini, N.; Bellucci, S.; Magrini, A.; Bergamaschi, A.; Mustelin, T., Multi-walled carbon nanotubes induce T lymphocyte apoptosis. *Toxicol. Lett.* **2006**, *160*, 121-126. DOI: 10.1016/j.toxlet.2005.06.020.

[27] Seifert, G.; Fowler, P.; Mitchell, D.; Porezag, D.; Frauenheim, T., Boron-nitrogen analogues of the fullerenes: electronic and structural properties. *Chem. Phys. Lett*. **1997**, *268*, 352-358. DOI: 10.1016/S0009-2614(97)00214-5.

[28] Matxain, J. M.; Eriksson, L. A.; Mercero, J. M.; Lopez, X.; Piris, M.; Ugalde, J. M.; Poater, J.; Matito, E.; Solá, M., New solids based on $B_{12}N_{12}$ fullerenes. *J. Phys. Chem. C* **2007**, *111*, 13354-13360. DOI: 10.1021/jp073773j.

[29] Oku, T.; Nishiwaki, A.; Narita, I., Formation and atomic structure of $B_{12}N_{12}$ nanocage clusters studied by mass spectrometry and cluster calculation. *Sci Technol. Adv. Mat*. **2004**, *5*, 635-638. DOI: 10.1016/j.stam.2004.03.017.

[30] Baei, M. T.; Taghartapeh, M. R.; Lemeski, E. T.; Soltani, A., A computational study of adenine, uracil, and cytosine adsorption upon AlN and BN nanocages. *Phys. Rev. B: Condens. Matter*. **2014**, *444*, 6-13. DOI: 10.1016/j.physb.2014.03.013.

[31] Chermahini, A. N.; Teimouri, A.; Farrokhpour, H., Theoretical studies of urea adsorption on single wall boron-nitride nanotubes. *Appl. Surf. Sci.* **2014**, *320*, 231-236. DOI: 10.1016/j.apsusc.2014.09.066.

[32] Rimola, A.; Sodupe, M., Gas-phase and microsolvated glycine interacting with boron nitride nanotubes. *A B3LYP-D2* Periodic Study. Inorganics* **2014**, *2*, 334-350.

[33] Rimola, A., Intrinsic ladders of affinity for amino-acid-analogues on boron nitride nanomaterials: A B3LYP-D2* periodic study. *J. Phys. Chem. C* **2015**, *119*, 17707-17717

[34] Lin, Q.; Zou, X.; Zhou, G.; Liu, R.; Wu, J.; Li, J.; Duan, W., Adsorption of DNA/RNA nucleobases on hexagonal boron nitride sheet: an ab initio study. *Phys Chem. Chem. Phys*. **2011**, *13*, 12225-12230. DOI: 10.1039/C1CP20783K.

[35] Ganji, M.; Yazdani, H.; Mirnejad, A., $B_{36}N_{36}$ Fullerene-like nanocages: a novel material for drug delivery. *Physica E* **2010**, *42*, 2184-2189. DOI: 10.1016/j.physe.2010.04.018.

[36] Mukhopadhyay, S.; Scheicher, R. H.; Pandey, R.; Karna, S. P., Sensitivity of boron nitride nanotubes toward biomolecules of different polarities. *J Phys Chem. Lett*. **2011**, *2*, 2442-2447. DOI: 10.1021/jz2010557.

[37] Rimola, A.; Sodupe, M., Physisorption *vs.* chemisorption of probe molecules on boron nitride nanomaterials: the effect of surface curvature. *Phys*.

Chem. Chem. Phys. **2013**, *15*, 13190-13198. DOI: 10.1039/C3CP51728D.

[38] Wu, X.; An, W.; Zeng, X. C., Chemical functionalization of boron-nitride nanotubes with NH_3 and amino functional groups. *J. Am. Chem. Soc.* 2006, *128*, 12001-12006. DOI: 10.1021/ja06365.

[39] Saini, S.; Hall, G. F.; Downs, M. E., Turner, A. P., Organic phase enzyme electrodes. *Anal. Chimica Acta* **1991**, *249*, 1-15. DOI: 10.1016/0003-2670(91)87002-O.

[40] Hall, G. F.; Best, D. J., Turner, A. P., The determination of p-cresol in chloroform with an enzyme electrode used in the organic phase. *Anal. Chimica Acta* **1988**, 213113-119. DOI: 10.1016/ S0003-2670(00)81345-8.

[41] Frisch, M.; Trucks, G.; Schlegel, H.; Scuseria, G.; Robb, M.; Cheeseman, J.; Montgomery Jr, J.; Vreven, T.; Kudin, K.; Burant, J., Pittsburgh PA, Pople JA (2009) Gaussian 09, revision A02. Gaussian Inc., Wallingford.

[42] MARTIN, J., Some observations and case studies on basis set convergence in density functional theory. 1999.

[43] Grimme, S., Semiempirical GGA-type density functional constructed with a long-range dispersion correction. *J. Comput. Chem.* **2006**, *27*, 1787-1799.

[44] Cossi, M.; Barone, V.; Mennucci, B.; Tomasi, J., *Ab initio* study of ionic solutions by a polarizable continuum dielectric model. *Chem. Phys. lett.* **1998**, *286*, 253-260. DOI: 10.1016/S0009-2614(98)00106-7.

[45] Barone, V.; Cossi, M.; Tomasi, J., Geometry optimization of molecular structures in solution by the polarizable continuum model. *J. Comput. Chem.* **1998**, *19*, 404-417. DOI: 10.1002/(SICI)1096-987X(199803)19:4<404::AID-JCC3>3.0.CO;2-W.

[46] Reed, A. E.; Weinstock, R. B.; Weinhold, F., Natural population analysis. *J. Chem. Phys.* **1985**, *83*, 735-746. DOI: 10.1063/1.449486.

[47] Geerlings, P.; De Proft, F.; Langenaeker, W., Conceptual density functional theory. *Chem. Rev.* **2003**, *103*, 1793-1874. DOI: 10.1021/cr990029p.

[48] Turi, L.; Dannenberg, J., Correcting for basis set superposition error in aggregates containing more than two molecules: ambiguities in the calculation of the counterpoise correction. *J. Phys. Chem.* **1993**, *97*, 2488-2490. DOI: 10.1021/j100113a002.

[49] O'boyle, N. M.; Tenderholt, A. L.; Langner, K. M., Cclib: a library for package-independent computational chemistry algorithms. *J. Comput. Chem.* **2008**, *29*, 839-845. DOI: 10.1002/jcc.20823.

[50] Johnson, E. R.; Keinan, S.; Mori-S Nchez, P.; Contreras-Garcia, J.; Cohen, A. J.; Yang, W., Revealing noncovalent interactions. *J. Am. Chem. Soc.* **2010**, *132*, 6498-6506. DOI: 10.1021/ja100936w.

[51] Lu, T.; Chen, F., Multiwfn: a multifunctional wavefunction analyzer. *J. Comput. Chem.* **2012**, *33*, 580-592. DOI: 10.1002/jcc.22885.

[52] Fernholt, L.; Romming, C., Molecular struture of gaseous pyrimidine. *Acta Chem. Scand. A* **1978**, *32*, 271-273. DOI: 10.3891/acta.chem.scand.32a-0271.

[53] Lan, Y. -Z.; Cheng, W. -D.; Wu, D. -S.; Li, X. -D.; Zhang, H.; Gong, Y. -J.; Shen, J.; Li, F. -F., Theoretical studies of third-order nonlinear optical response for $B_{12}N_{12}$, $B_{24}N_{24}$ and $B_{36}N_{36}$ clusters. *J. Mol. Struct.* **2005**, *730*, 9-15. DOI: 10.1016/ j.theochem.2005.06.008.

[54] Bahrami, A.; Seidi, S.; Baheri, T.; Aghamohammadi, M., A first-principles study on the adsorption behavior of amphetamine on pristine, P- and Al-doped $B_{12}N_{12}$ nano-cages. *Superlattices Microstruct.* **2013**, *64*, 265-273. DOI: 10.1016/j.spmi.2013.09.034.

[55] Esrafili, M. D.; Nurazar, R., A density functional theory study on the adsorption and decomposition of methanol on $B_{12}N_{12}$ fullerene-like nanocage. *Superlattices Microstruct.* **2014**, *67*, 54-60. DOI: 10.1016/j.spmi.2013.12.020.

[56] Peymani, S.; Izadyar, M.; Nakhaeipour, A., Functionalization of the single-walled carbon nanotubes by sulfur dioxide and electric field effect, a theoretical study on the mechanism. *Phys. Chem. Res.* **2016**, *4*, 553-565, DOI: 10.22036/pcr.2016.15614.

[57] Izadyar, M.; Khavani, M., Selective binding of cyclic nanopeptide with halides and ion pairs; a DFT-D3 Study. *Phys. Chem. Res.* **2017**, *5*, 425-437, DOI:

10.22036/pcr.2017.67519.1323.

[58] Izadyar, M.; Khavani, M.; Housaindokht, M. R., Sensing ability of hybrid cyclic nanopeptides based on thiourea cryptands for different ions, A joint DFT-D3/MD study. *J. Phys. Chem. A* **2017**, *121*, 244-255, DOI: 10.1021/acs.jpca.6b09738.

[59] Sabet-Sarvestani, H.; Eshghi, H.; Izadyar, M.; Bakavoli, M., NCI concept as a powerful tool to investigate the origin of Diels-Alder reaction accelerating inside the self-assembled softball nanoreactor. *J. Incl. Phenom. Macrocycl. Chem.* **2016**, *85*, 237-246, DOI: 10.1007/s10847-016-0623-2.

[60] Javan, M. B.; Soltani, A.; Azmoodeh, Z.; Abdolahi, N.; Gholami, N., A DFT study on the interaction between 5-fluorouracil and $B_{12}N_{12}$ nanocluster. *RSC Adv.* **2016**, *6*, 104513-104521, DOI: 10.1039/C6RA18196A.